



HAL
open science

Infrared Spectroscopy: Classical Methods

Jacques Saussey, Frederic Thibault-Starzyk

► **To cite this version:**

Jacques Saussey, Frederic Thibault-Starzyk. Infrared Spectroscopy: Classical Methods. Bert Marc Weckhuysen. In Situ Characterization of Catalysts, American Scientific Publishers, pp.15-31, 2004, 1-58883-026-8. hal-04661179

HAL Id: hal-04661179

<https://hal.science/hal-04661179v1>

Submitted on 25 Jul 2024

HAL is a multi-disciplinary open access archive for the deposit and dissemination of scientific research documents, whether they are published or not. The documents may come from teaching and research institutions in France or abroad, or from public or private research centers.

L'archive ouverte pluridisciplinaire **HAL**, est destinée au dépôt et à la diffusion de documents scientifiques de niveau recherche, publiés ou non, émanant des établissements d'enseignement et de recherche français ou étrangers, des laboratoires publics ou privés.

Infrared Spectroscopy: Classical Methods

Jacques Saussey & Frederic Thibault-Starzyk

Catalysis and Spectrochemistry Laboratory, Université de Caen, CNRS-ISMRA,

6 Boulevard Maréchal Juin, 14050 Caen, France

fts@ismra.fr

Introduction

Operando infrared spectroscopy is the infrared monitoring of the surface of a working catalyst, most often combined with on-line analysis of the reaction products. It dates back to the end of the sixties [1], but observation of the infrared light coming through a self-supporting disc of powder was a difficult task at that time. It was made much easier by the introduction of modern Fourier transform spectrometers, by the introduction of improved sensitivity detectors, and by other sampling techniques such as diffuse reflection. The reasonable price of modern spectrometers makes infrared spectroscopy available to most heterogeneous catalysis laboratories. It is therefore not surprising that the amount of publications dealing with “in situ” infrared spectroscopy has steadily increased. Recently, a lengthy review was published on this topic [2]. Experimental conditions are however most of the time very different to those of the real reaction, and the number of articles describing operando infrared spectroscopy is not that substantial. The surface of the catalyst is very different from the surface of the activated fresh catalyst under vacuum (as we will see later in this chapter), and observing the working catalyst in real reaction conditions is critical.

Although it was ambiguously called *in situ*, *operando* infrared spectroscopy has progressed considerably since its origin. In 1991, volume 9 of *Catalysis Today* grouped 28 papers after a meeting on “*in situ* methods in catalysis” in United Kingdom. Out of these 28 contributions, 10 dealt with *operando* infrared spectroscopy and gave state-of-the-art perspectives. The technique was reaching maturity, but observed phenomena were complex and conclusions were hardly general. The number of research groups working in the domain has since increased, and a recent review of all *operando* techniques (establishing the name of the method) showed infrared is still one of the major tools in this field [3]. The technique is always improving. Still new cells appear to overcome the experimental limits: problem of the microreactor for kinetic studies [4], using fixed bed rather than wafers [5], or to explore the domain of liquid/solid heterogeneous systems [6, 7]. It should be noticed that the now classical cell of Bell [8] is still in use, for example for studying methanol synthesis [9]. The infrared reactor-cell is not always coupled with on-line analysis of the reaction products (although it is a requirement for using the term *operando*), but can be compared with reactors without infrared monitoring, for example in deNO_x studies [10], or only for observing surface species [11].

Many aspects of heterogeneous catalysis can be treated, from deactivation and coke formation [12, 13, 14] to the identification of intermediate species [15, 16] and determination of the mechanism by reaction kinetics (combining the kinetics of surface processes with the usual time change analysis of the reaction products in the gas phase). Kinetics have even been studied by imposing periodic variations of reactant concentrations [17], creating a sort of imposed oscillatory reaction (which has also been studied on its own by *operando* infrared [18]).

Here, we want to give the reader a clear picture of what is really within reach of operando infrared. We will try to give a critical view and provide a systematic approach of heterogeneous catalysis by operando infrared spectroscopy.

Experimental aspects

Infrared spectroscopy can be performed by two separate technical modes, transmission of the light through the sample or collection of the light diffused by the surface of the powder. While diffuse reflection cells are commercially available and are quickly spreading over catalysis laboratories, transmission cells are more difficult to design for catalytic studies and are usually home made. However, they offer several important advantages over the diffuse reflection cells. The first advantage is for quantitative studies, since transmission infrared mostly obeys Beer-Lambert's law (although it is not rigorous for powdered solids). Diffuse reflection spectroscopy follows Kubelka-Munk's theory and band intensities are strongly influenced by the size of the grains, the temperature and depend very much on reaction conditions.

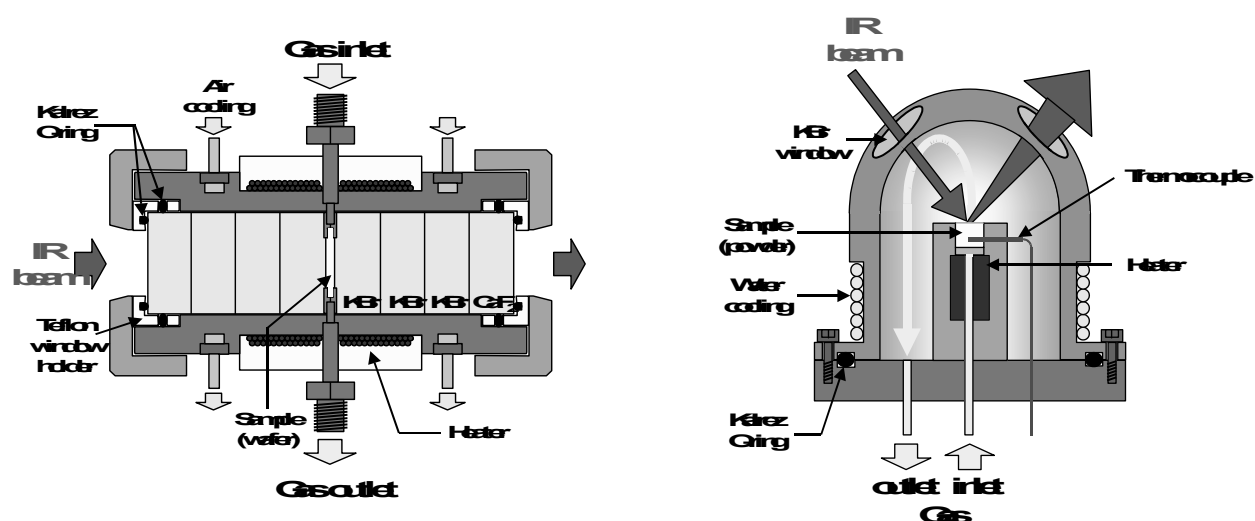


Figure 1: Left: home-made transmission cell used in the Catalysis and Spectrochemistry Laboratory in Caen; Right: commercial diffuse reflection cell.

The second main difference between both types of spectroscopies is the cell's behaviour as a chemical reactor. In the transmission cell, the catalyst powder is pressed into a self-supporting wafer along which the reactant gas flows. In the diffuse reflection cell, the catalyst powder is placed (and slightly pressed) in a cup, through which the gas flows: this seems to give this second cell a definite advantage over the first (for gas diffusion through the bed), but we will show that the case is not so simple.

The transmission cell can be built with a very narrow sample holder, leaving only a very small dead volume between the wafer and the walls (KBr windows), and leading to an improved ratio between the gas/wafer interface and the dead volume. This very narrow space between the catalyst and the infrared windows leaves only a very narrow space for the gas phase in the optical path. The gas contribution to the operando spectrum is therefore very small, even at high pressure. Moreover, the wafer can be in the heart of a homogeneous heating block with a very small temperature gradient and good temperature control. Commercial DRS cells have three main drawbacks:

- the important temperature gradient between the observed surface and the bottom of the cup.
- the infrared analysis only takes into account the top of the catalyst bed and differences are often noticed between the observed reactivity as viewed by the infrared spectrum and by on-line analysis techniques (GC, ...). The reaction can be more important at the bottom of the catalyst bed (where the temperature might be much higher than on the surface of the bed) than on the surface observed by infrared.
- the important dead volume in the catalytic chamber: the contact time of the reactants is important and the time resolution of pulsed experiments is low. The gas phase can also contribute strongly to the infrared spectra.

When both techniques are available, the use of transmission is strongly advised whenever the catalyst can be put in the form of a wafer and the temperature does not need to be higher than 700 K (some transmission cells are claimed to have no limit [¹⁹]).

The infrared cell is placed in a gas line with a reactant gas flow and on-line analysis of the products. The design is optimised to have the smallest possible dead volume and fast time resolution in transient perturbations. Such a setting allows on-line analysis of products at 1 s time resolution by an infrared gas cell or by a mass spectrometer. Both techniques can be used continuously or synchronised with the analysis of surface species. An injection loop is used to send in the reactor very small amounts of the reactant (5 to 50 μl of gas) for micro reactivity or use of probe molecules on the working catalyst.

A systematic approach

Operando spectroscopy mainly aims at determining reaction mechanisms and intermediates. The simplest chemical reaction is the transformation of a reactant into a product via an intermediate step denoted as, depending on its lifetime,

- transition states $t \sim 10^{-13}\text{s}$
- intermediate species $t > 10^{-12}\text{s}$.

In most cases, the global reaction is a sequence of such elementary reactions. When an intermediate species is involved, it is possible to determine some of its structural and reaction properties. Two theoretical approaches are used to relate the surface concentrations with the gas phase pressure: Langmuir's uses only identical sites, while Temkin's approach deals with various sites as a function of the loading. To apply such formalisms, an equilibrium between the gas and the adsorbed phases is needed. Therefore, adsorption must not be the limiting step.

The heterogeneous catalysed process can be divided into five separate steps:

- reactants diffusion: gas molecules have to diffuse towards the surface sites where the reaction will take place. Infrared allows one to follow the fast penetration of molecules in the pores (e.g. for zeolites).
- adsorption of the reactants: most of the time, infrared spectroscopy can be used to characterise the type of adsorption, the way the molecule is attached and the adsorption site.
- surface reaction: this is usually a chain of fast elementary reaction steps. One slow step (or a combination of several) can control the global reaction speed. Differentiation of active intermediates among spectator species is difficult, therefore coupling of infrared with on-line analytical techniques such as gas chromatography or mass spectroscopy is needed.
- desorption of reaction products.
- diffusion of products: gas molecules lead the catalyst toward the open gas phase.

The reaction mechanism corresponds to these five steps. The conditions are usually chosen to avoid the influence of diffusion on the reaction kinetics.

Establishing a general approach for the study of catalytic reactions by in situ infrared spectroscopy is a difficult task because spectral information obtained differs from one reaction to another. In some cases, many bands are observed, while in other cases, nothing is visible. Studying reaction mechanisms enables the collection of as much information as possible on the reaction process in steady state, but also in transient conditions. The results obtained will mainly reflect the whole reaction pathway, but some elementary steps will also be identified. The first task in the study will always be to identify all the species detected in steady state. If the adsorbed mixture gets more complicated with time, this identification has

to be done in the transient regime of the beginning of the reaction. Adsorbed reactants (first intermediates) are usually easy to characterise. Adsorbed final reaction products (final intermediates) are less often present in the spectrum of the adsorbed species. Adsorbed intermediates, between those two extreme steps, are more difficult to characterise, unless they occur just before a slow limiting step. Establishing the role of such an adsorbed species as a reaction intermediate in the mechanism is only possible by coupling surface infrared spectroscopy and on-line analysis of the catalyst activity.

1) Characterisation of surface species

The spectrum can be complicated by the presence of many chemical species in the reactor-cell. If the gas pressure is high, and if the infrared absorption of the reactant is strong, the spectrum of the gas phase and physisorbed reactant will be intense. Chemical species can be in three states in the cell:

- a **gas** will often lead to broad bands, with sometimes a fine rotational substructure (depending on the resolution) with two or three components. The intensity is proportional to the pressure in the cell.

- the spectrum of a **physisorbed species** is generally very similar to that of the corresponding liquid. Wavenumbers are very close. These physisorbed species do not appear very often since they need partial pressure and temperature conditions near the gas-liquid equilibrium state. In zeolites, confinement in the pores enhances physical adsorption and pseudo-liquid state is observed more often.

- the spectrum of a **chemisorbed species** is perturbed in various degrees, depending on its dissociative or non-dissociative adsorption. Chemical bonds will be more perturbed if they are close to the anchoring point of the catalyst. Vibration involving these bonds will then differ much from the homologous vibrations of the same compound in the liquid state.

Preliminary experiments will give very useful information to understand the real in situ study. Several spectra will be recorded prior to the study of the real working conditions. In the case of metal supported catalysts for example, the bare support will first be studied, then the support together with the metal after activation, and the spectrum of the pure gas phase (reactant without catalyst). The reaction will also be first performed on the catalyst support without metal. To determine the structure of the chemisorbed species, the band shifts of the surface functional groups (generally OH groups) and of the reactant vibrations will provide useful information. In many cases, the interaction will be of the acid-base type with an OH group on the surface and an organic function on the adsorbed reactant.

a) Butyne on Pt/SiO₂

The reduction of butyne on Pt/SiO₂ (to form butene and butane) [20] will provide the first example of such a systematic study for the determination of surface species. In the case of but-1-yne adsorption on pure silica (Fig. 2), the molecule contains a weakly acidic proton and an electron rich (basic) triple bond.

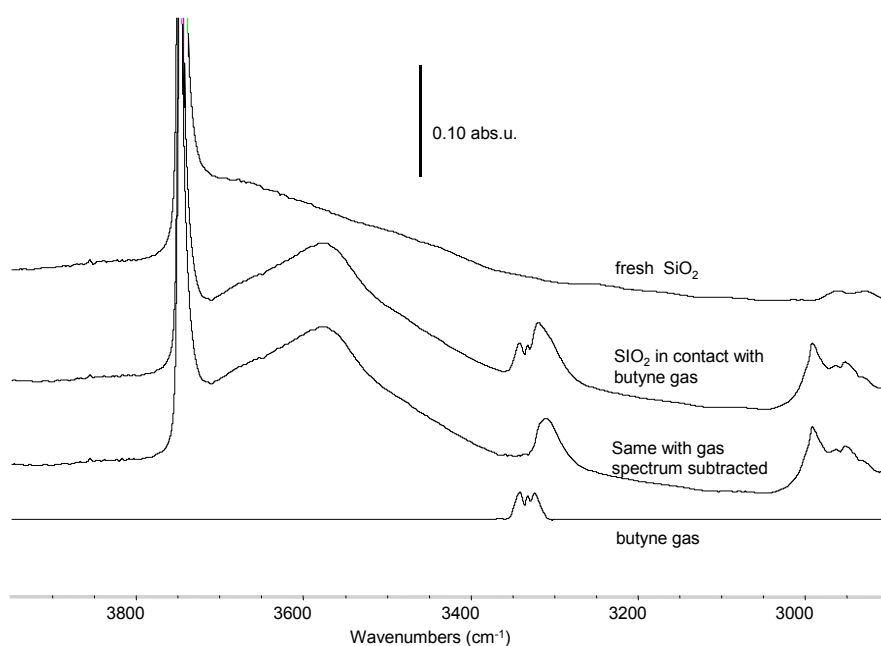


Figure 2: spectra of silica under a butyne (14 torr) + H₂ (38 torr) flow at 300 K.

The surface silanol presents a weakly acidic proton and an electron rich oxygen. However, if the pKa of the silanol group is higher than that of the alkyne group (the silanol is the stronger acid), butyne then plays the role of the base in the interaction, and the $\nu(\text{OH})$ vibration shifts to lower wavenumbers. If the opposite were true, the $\nu(\equiv\text{C-H})$ vibration in the butyne would shift 150-200 cm^{-1} to lower wavenumbers. The influence of the surface binding on the molecule vibrations can be seen in table 1.

Table 1: infrared absorption bands of 1-butyne in the pure (gas or liquid state) or adsorbed state (frequencies are given in cm^{-1}). Vibrations which are the most distant from the anchoring point to the surface are only slightly perturbed.

	gas phase	liquid	chemisorbed
$\nu(\text{CH})$	3332	3315	3310
$\nu(\text{CC})$	2132	2120	2115
$\nu_a(\text{CH}_3)$	2991	2982	2991
$\nu_s(\text{CH}_3)$	2953	2941	~2952
$\nu(\text{CH}_2)$	2939	2923	~2926

On the surface of silica with supported Pt, butyne concentration is not as high. Because the reaction is fast, it is reduced into butane. When the catalyst deactivates, the amount of surface adsorbed butyne increases again, and the selectivity is modified. Butyne is then preferentially converted into butene.

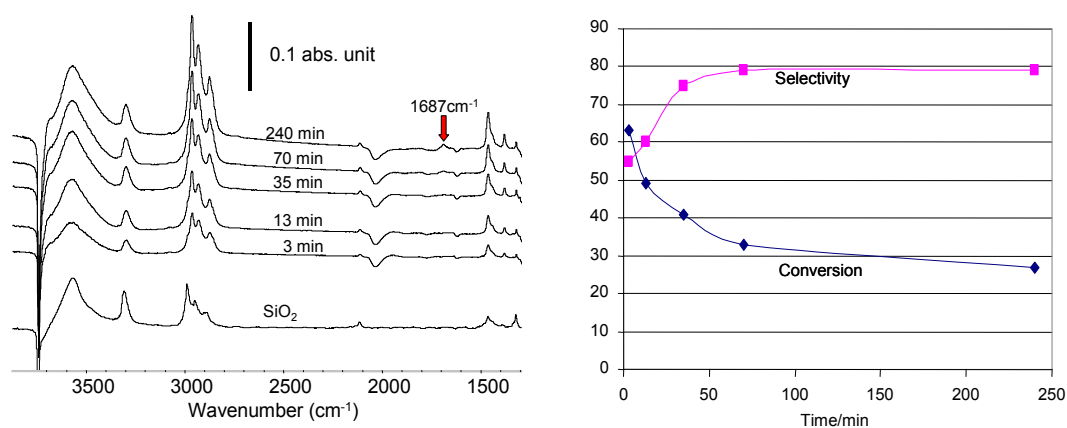


Figure 3: spectra of Pt/SiO₂ (2.7% Pt) under a butyne (14 torr) + H₂ (38 torr) flow at 300 K. The amount of butyne is lower than on pure silica because of its fast conversion (mainly into butane).

When silanols coverage by butyne reaches one, the reaction is completely selective for butene: butyne on the silanols can be quickly transferred to the Pt sites, thus preventing the dissociative adsorption of H₂ that would lead to total hydrogenation into butane. On platinum, butyne forms a di-σ species, detected by a weak band at 1687 cm⁻¹, which was assigned by comparison with the corresponding organo-metal complex.

b) Methylbutynol decomposition on MgO

3-Methyl-1-butyne-3-ol is a test molecule for the determination of the basic, acid or amphoteric properties of a surface, producing various reaction products:

- methylbutyne and prenal on an acidic surface
- hydroxymethylbutanone on an amphoteric surface
- acetone and ethyne on a basic surface.

Methylbutynol is thus a molecule of choice for the study of the structure of adsorbed species by in situ infrared. Both organic functions of the molecule can interact with the surface. The most acidic function is the OH group, it is the preferred interaction point, leading to the OH

associated form or to the species obtained by dissociation of the OH, with the yne function free or interacting in the case of basic or amphoteric surfaces.

Figure 4 displays the spectra of MgO at 450 K under a methylbutynol flow. Two species are observed on the surface from the beginning, mainly characterised by $\nu(\text{C-O})$ and $\nu(\equiv\text{CH})$ vibration bands. The vibrations at 963 cm^{-1} ($\nu(\text{C-O})$) and 3316 cm^{-1} ($\nu(\equiv\text{C-H})$) point to a H-bonded methylbutynol, interacting via the OH group to the oxygen of the oxide surface. The $\equiv\text{CH}$ remains free. The vibrations at 3206 and 1001 cm^{-1} in the second species (second independent set of bands) are assigned to dissociated methylbutynol, interacting with the surface via the $\equiv\text{CH}$. This specific interaction takes place because of the oxygen atoms being strongly basic. It is not observed on alumina, where the ethynic proton is not interacting with the surface in the dissociated species. After the first moments, the spectra rapidly get more complicated, because acetone is produced in the reaction and oligomerises on the surface.

Quantum calculations were used to show the modifications of the electronic densities on the surface by bonding to methylbutynol, depending on the type of surface. On zirconia [21], the empty d orbitals of zirconium play a crucial role. Once methylbutynol is adsorbed under the form of an alkoxide, a charge transfer takes place and allows the nucleophilic attack on the other carbon atom of the triple bond.

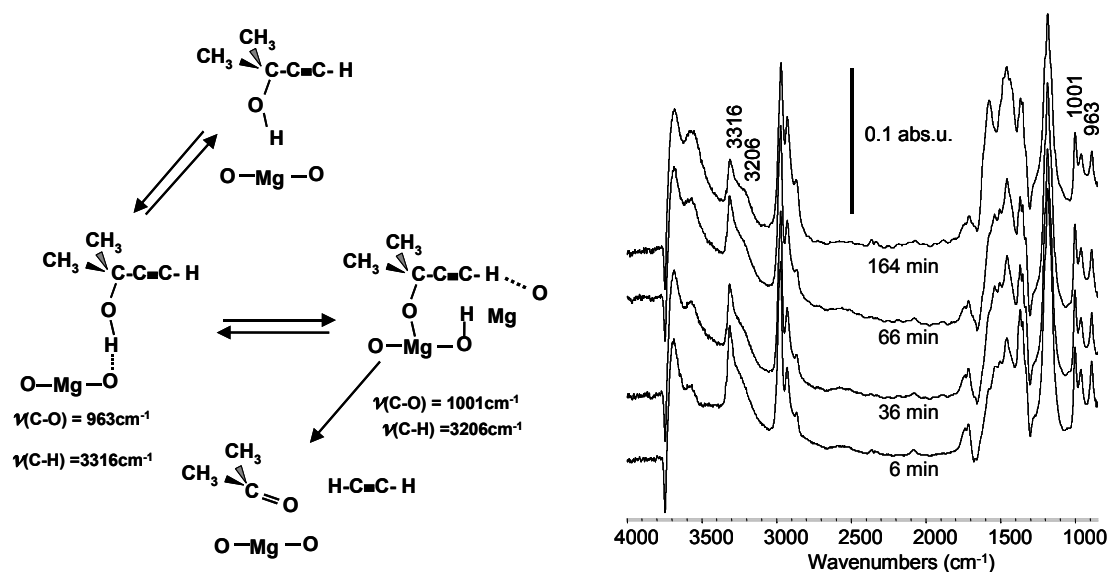


Figure 4: surface species observed during methylbutynol decomposition on MgO at 450 K.

c) Salicylic acid on silica

Figure 5 shows the spectra recorded during adsorption of salicylic acid on silica in a flow of hydrogen. Salicylic acid has two organic functions (carboxylic and hydroxy groups), thus its adsorption on the surface is a nice case study. Like most carboxylic acids, and due to the intermolecular H-bonding, salicylic acid is at room temperature under the form of a mixture of monomer ($\nu(\text{CO})$ at 1698 cm^{-1}) and dimer ($\nu(\text{CO})$ at 1663 cm^{-1}). At 573 K, the monomer is present in the gas phase only under atmospheric pressure. In the monomer, an intramolecular H-bond can form between the phenolic OH group and the carboxylic group, the hydrogen donor being either the OH group or the carboxylic group. By comparing with the spectrum of methyl salicylate, and with that of methoxymethylsalicylate, we can determine the frequency of the free C=O vibration: it was assigned to 1760 cm^{-1} . The H-bond C=O groups vibrates at 1684 cm^{-1} . This assignment was used to determine the intramolecular conformation of salicylic acid, in which the C=O at 1698 cm^{-1} indicates a H-bonding between the phenolic OH (proton donor) and the C=O moiety of the carboxylic group (proton acceptor).

On the surface of silica, the adsorption leads to the nearly complete and fast disappearance of the silanols groups. The first adsorbed species has two main vibration bands at 1594 and 1494 cm^{-1} , with no visible $\nu(\text{C}=\text{O})$ vibration. This is indicative of phenol dissociatively adsorbed on the surface, formed by the thermal decarboxylation of salicylic acid.

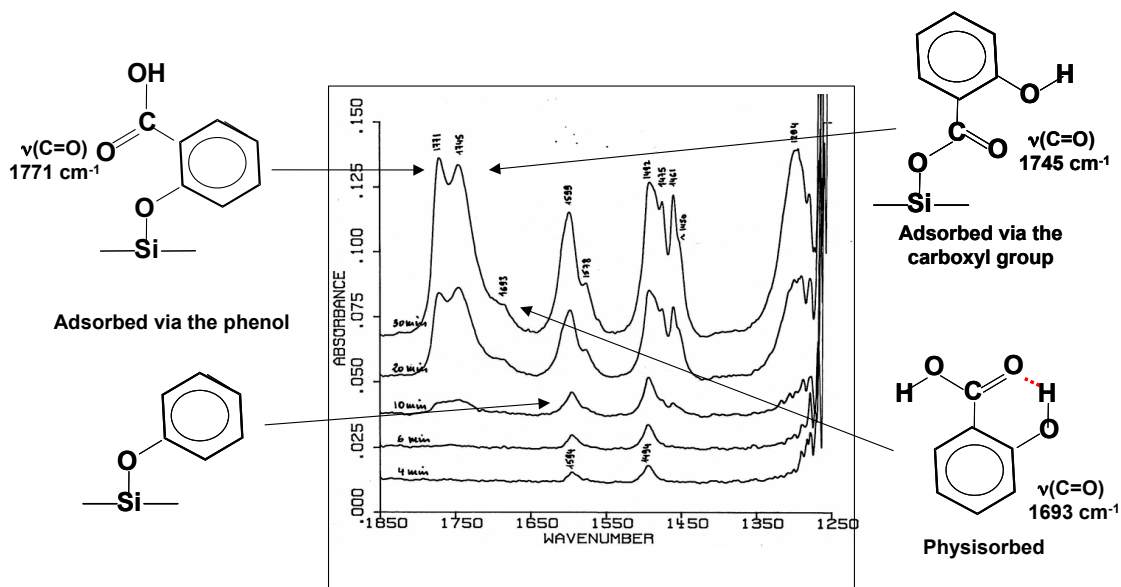


Figure 5: adsorption of salicylic acid (2 torr in a H_2 flow at atmospheric pressure) on silica at 573 K.

In a second step, two other species appear in the adsorbed state, with $\nu(\text{C}=\text{O})$ vibration bands at 1771 and 1745 cm^{-1} , indicating free $\text{C}=\text{O}$ groups. The first species is bound to the surface through its phenolic OH group, the second one through the carboxylic OH. One of these two is probably the intermediate to the decarboxylated species already detected (it is only detected when the reaction starts slowing down). The last species to appear on the surface is similar to the monomeric salicylic acid, with $\nu(\text{C}=\text{O})$ at 1693 cm^{-1} . This is the physisorbed molecule.

2) Identification of intermediate species

After surface species have been identified, the next step is to determine which is a reaction intermediate, and which is only a spectator species or the product of a side reaction.

According to the Langmuir-Hinshelwood theory, the surface elementary reaction rate is proportional to the surface concentration of the adsorbed species involved in the reaction process. An increase of this concentration will result in a corresponding increase of the reaction speed. Inversely, any change affecting the reaction speed will modify the surface concentration of the intermediate surface species. The reactant pressure is generally an effective way for such a perturbation. Pulses of the reactant can be sent to the flow, and the shape of the variation of the infrared absorbance ought to follow the reactant partial pressure. Fast and efficient analysis techniques will always be necessary to follow these transient systems, using for example an infrared gas cell, mass spectroscopy or a fast micro-GC.

a) Synthesis of methanol from CO

Carbon monoxide on metal has been the source of many different research topics in infrared spectroscopy because it leads to intense $\nu(\text{C}\equiv\text{O})$ absorption bands, which are easy to use for the identification of the various adsorption modes on the metal. However, the determination of real reaction intermediates in the synthesis of methanol from CO and H₂ is not straightforward, as many surface species appear on the catalyst: carbonyls and formates, as well as carbonates and methoxy groups on occasion. This reaction has been studied on zinc aluminate supported copper catalysts, and it is a very good example of the combined use of operando spectroscopy and on-line analysis for the determination of mechanism and reaction intermediates [22]. The reaction is performed under 10 bar of a H₂ and CO mixture at 250°C. Surface species are monitored by transmission infrared spectroscopy, while reaction products coming out of the reactor are analysed by on-line gas chromatography.

Two types of formate species (type I and II) exist on the solid support. They can be studied by the first overtone of their vibration (very clear and resolved bands, but with very weak

intensity). On the bare support (0% Cu catalyst), this very weak overtone has been used when studying the reaction, thus showing the sensitivity of the technique even at high pressure.

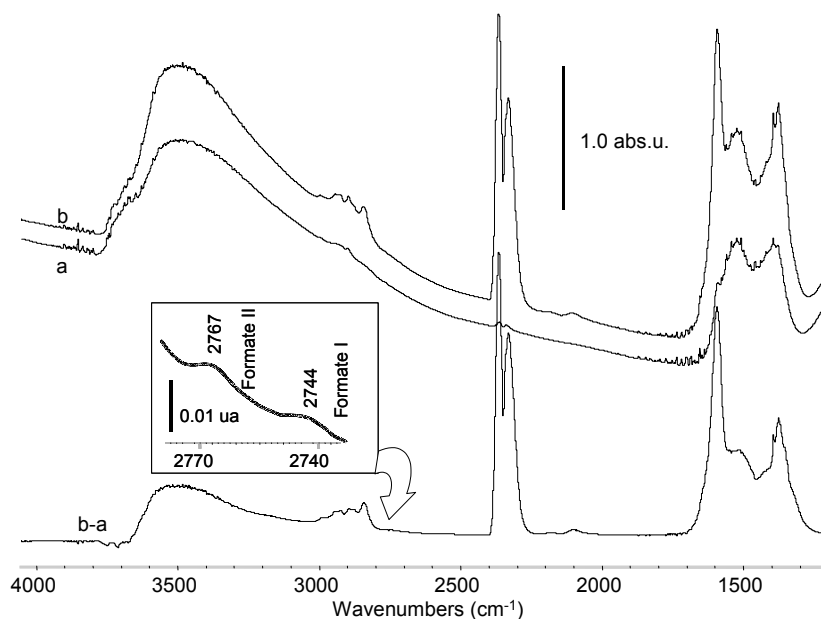


Figure 6: spectra recorded during the hydrogenation of CO on Cu/ZnAl₂O₄ at 250 C. a) activated catalyst; b) catalyst under 10 bar gas flow. b-a shows modifications: at 1100 cm⁻¹, the surface methoxy groups; between 1200 and 1700 cm⁻¹, overlapping formates and carbonates bands; between 2700 and 3000 cm⁻¹, ν (CH) vibration bands; at 3500 cm⁻¹ and above, negative band due to the perturbation of surface OH groups. Inset: overtone bands of the formate vibration bands between 2700 and 2800 cm⁻¹.

The spectra on the active catalyst, Cu/ZnAl₂O₄, are shown in figure 6. Two separate reaction mechanisms are possible. Insertion of CO under a surface OH group can lead to surface formate groups, further converted into methoxy surface groups, and leading to methanol after hydrogenation. In the case of an active copper catalyst, neither copper formate nor copper methoxy species are detected: methoxy groups on the support only build up (in high amounts) on the surface. Desorption is the limiting step, and the methanol formation rate is linked to the product of surface concentrations of methoxy groups and hydrogen. Both species, methoxy groups on the support and hydrogen on copper, are located on two separate adsorption sites.

The second possible route is hydrogenation of copper carbonyls via formyl species. The corresponding kinetic equation is the product of surface concentrations of carbonyl groups and of hydrogen. To check which is the main mechanism, the approach used was to keep hydrogen partial pressure constant, while varying that of carbon monoxide. In the formate mechanism, the equation becomes very simple. The surface concentration of dissociated H_2 is constant and the reaction speed only depends on the surface methoxy groups concentration:

$$V_{MeOH} = k_1 [CH_3O] [H] = k_1' [CH_3O]$$

In the case of the carbonyl mechanism, the Langmuir-Hinshelwood theory leads to two equations, depending on the competitive or non-competitive adsorption of CO and hydrogen.

If the adsorption is non-competitive:

$$V_{MeOH} = k_2 [CO-Cu] [H] = k_2' \left[\frac{K_{CO} P_{CO}}{1 + K_{CO} P_{CO}} \right] \left[\frac{K_{H_2} P_{H_2}^{1/2}}{1 + K_{H_2} P_{H_2}^{1/2}} \right]$$

K_{CO} and K_{H_2} being the adsorption constants of both species on two separate sites. This equation is simplified if the hydrogen pressure is kept constant:

$$V_{MeOH} = k_2'' \frac{K_{CO} P_{CO}}{1 + K_{CO} P_{CO}}$$

For the competitive adsorption, the result is slightly different:

$$V_{MeOH} = k_2'' \frac{K_{CO} P_{CO}}{(1 + K_{CO} P_{CO})^2}$$

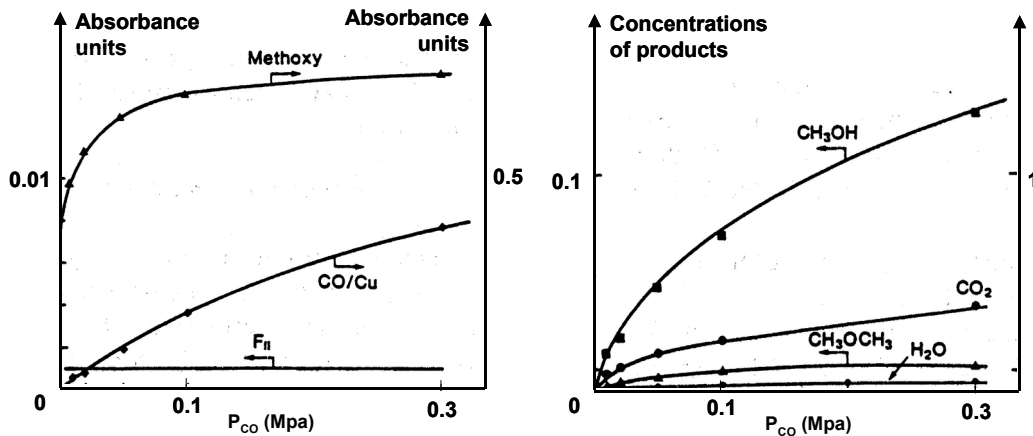


Figure 7: results obtained during the reaction at various CO partial pressure (250 C, $P_{H_2} = 0.7$ Mpa). Left: infrared intensity variations for adsorbed CH_3O and CO species on the catalyst surface. Right: relative amounts of reaction products coming out of the reactor.

The formate mechanism was easily excluded, since the surface methoxy concentration clearly was not linearly linked to the amount of methanol produced (fig. 7). Concerning the carbonyl route, K_{CO} was measured easily because the surface carbonyl concentration is directly linked to P_{CO} . The equations corresponding to the competitive and non-competitive adsorption were fit to the experimental point at the highest P_{CO} . A very nice fit was obtained for the competitive adsorption (fig. 8).

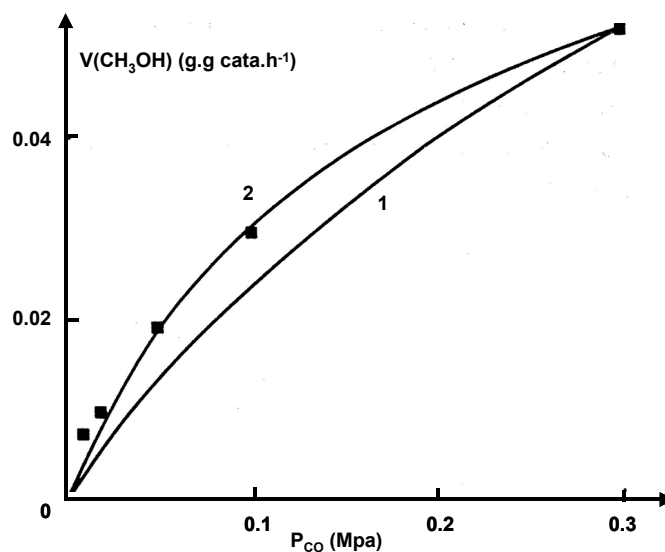


Figure 8: experimental (■) rates of methanol formation as a function of P_{CO} . Curve 1 computed assuming a non-competitive adsorption between CO and H₂, curve 2 computed assuming a competitive adsorption.

Thus, the reaction mechanism was determined together with the adsorption site. Combining surface and gas species in the kinetic modelling of the system is one of the most powerful approaches for operando spectroscopy.

b) Reaction of NO and CO on Pt/SiO₂

CO species on platinum were known to appear during the reduction of NO_x by hydrocarbon on silica-supported platinum. The surface concentration of these species seemed linked to the deNO_x activity, but the role was unknown. The role of CO in the reduction of NO_x on Pt catalyst was studied by operando IR spectroscopy, giving a good example of high time resolution for the understanding of surface processes [23].

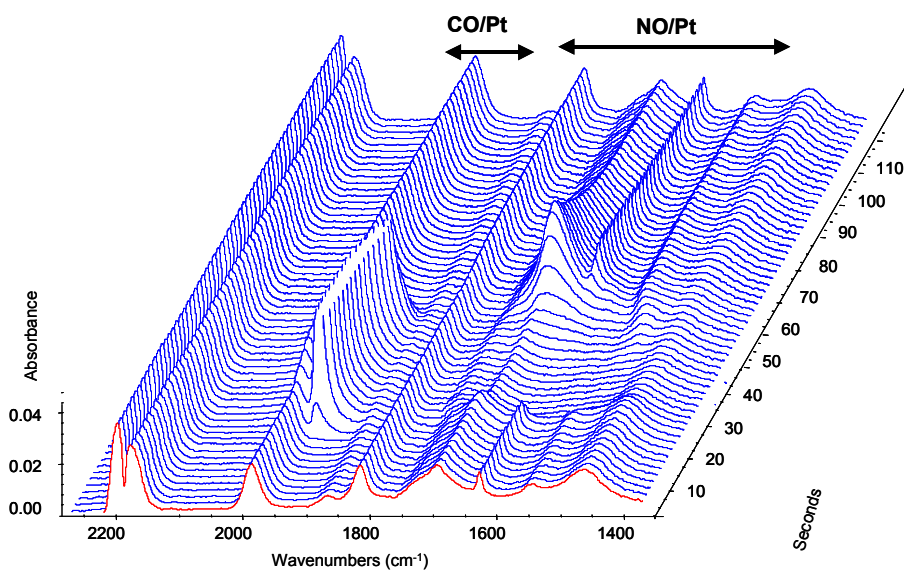


Figure 9: spectra of the surface of the working catalyst during NO_x reduction on Pt/SiO₂ (3.6% Pt, 250°C, 1000 ppm NO in 1 atm He flow). At 30 s time on stream, a 20 μL pulse of CO is injected in the flow.

The catalyst was first run in the reactor-cell with the normal reactants mixture in order for all adsorbed species to be present on the surface. Then, a flow of pure NO in the carrier gas was established on the catalyst. Several linearly adsorbed NO species were detected on oxidised platinum (NO_{lin}/Pt_{ox}), as well as nitrate species (fig. 9). Very stable CO species on the oxidised metal were also present (and inactive) on the surface. A CO pulse was sent in the

flow (see fig. 9, between 30 and 60 s), and linearly adsorbed CO on reduced platinum ($\text{CO}_{\text{lin}}/\text{Pt}_{\text{red}}$) appeared in high quantities. Simultaneously, most of $\text{NO}_{\text{lin}}/\text{Pt}_{\text{ox}}$ disappeared, together with nitrates (a new Pt-NCO appears transiently at maximum $\text{CO}_{\text{lin}}/\text{Pt}_{\text{red}}$ intensity, with a very weak band at 2181 cm^{-1}). As soon as $\text{CO}_{\text{lin}}/\text{Pt}_{\text{red}}$ disappears on the surface (fig. 9, at time 60 s), NO species come back with a slightly higher intensity at first (due to O_2 blocking some Pt sites).

At the same time, the gas phase was also monitored by infrared spectroscopy (fig. 10). Before the CO pulse, only NO and a small amount of NO_2 were present in the flow. During the pulse, CO_2 had two separate concentration maxima. At the first CO_2 maximum, a partial desorption of NO was observed. At the second maximum, NO and NO_2 were consumed, and N_2O was produced. After the pulse, NO came back to its initial concentration very rapidly, while NO_2 returned to its initial concentration in a later step. N_2 could not be observed in the IR cell, as mass spectroscopy was needed (fig. 12).

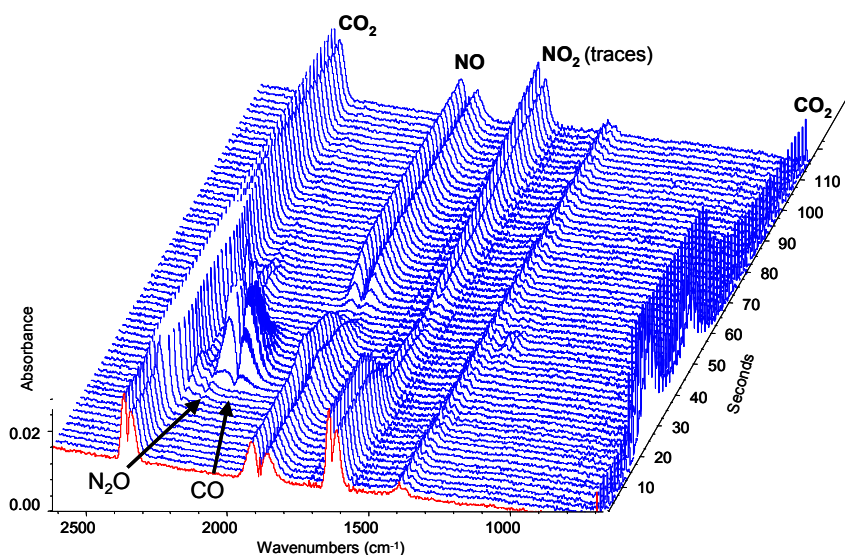


Figure 10: spectra of the gas phase coming out of the reactor during the NO_x reduction experiment on Pt/SiO_2 .

By comparing both time sequences, in the gas phase and on the surface (fig. 11), the reaction can be explained. Before the pulse, the surface is covered by linear NO, nitrates and PtO. Two

separate steps can be distinguished during the CO pulse. CO first consumes all oxygen on platinum, leading to the first CO₂ outcome in the gas phase. This initial combustion of CO might explain the NO desorption observed in the first step due to heating of the surface.

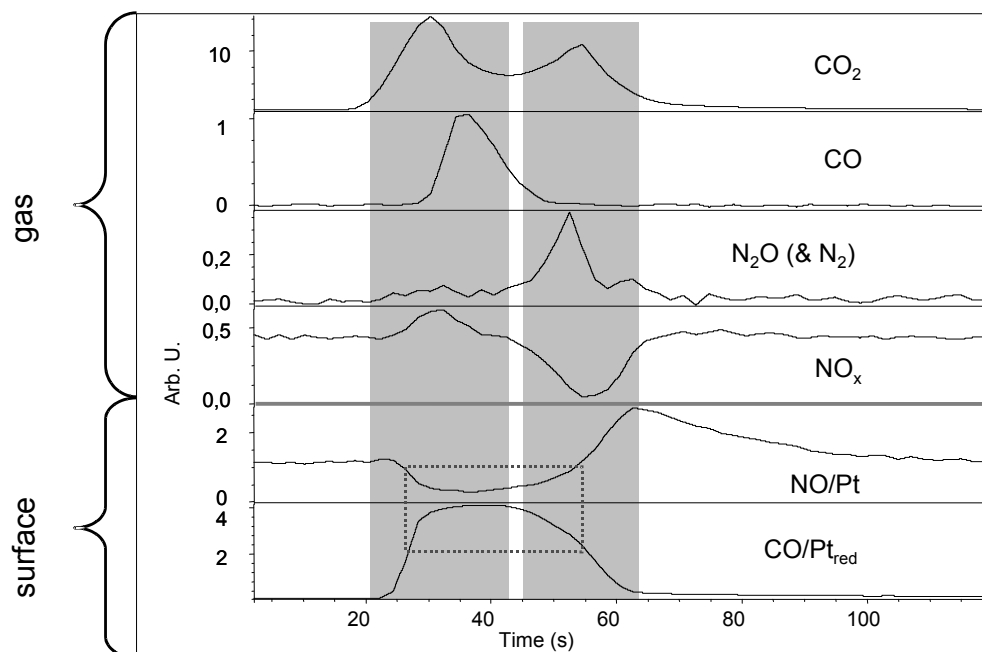


Figure 11: comparison of the two time sequences observed during the NO_x reduction experiment on Pt/SiO₂, on the surface and in the gas phase. The dotted rectangle indicates that CO and NO surface concentrations have the same values at 25 and 55 s.

When CO_{lin}/Pt_{red} reaches its maximum concentration, a lack of surface oxygen explains the decrease of CO₂ production. CO then progressively desorbs, leaving free reduced Pt sites for the dissociation of NO. This dissociation produces surface oxygen, leading to the second CO₂ formation peak, detected together with the formation of N₂O and N₂ (in the mass spectra) and the decrease of NO concentration.

This dissociative mechanism is evidenced by the difference in reaction products for same CO concentrations and the same NO concentrations, on both sides of the surface CO and NO peaks (25 and 55 s, dotted rectangle in fig. 11). If there were a direct reaction between both species, the products would be the same at both points.

Nitrogen in the gas phase cannot be detected by IR spectroscopy. It can be detected by mass spectroscopy, but CO has the same mass, and ^{15}NO isotopic labelling was needed to distinguish $^{15}\text{N}_2$ from CO in the gas. Together with the production of N_2O , a simultaneous and more intense production of N_2 was observed.

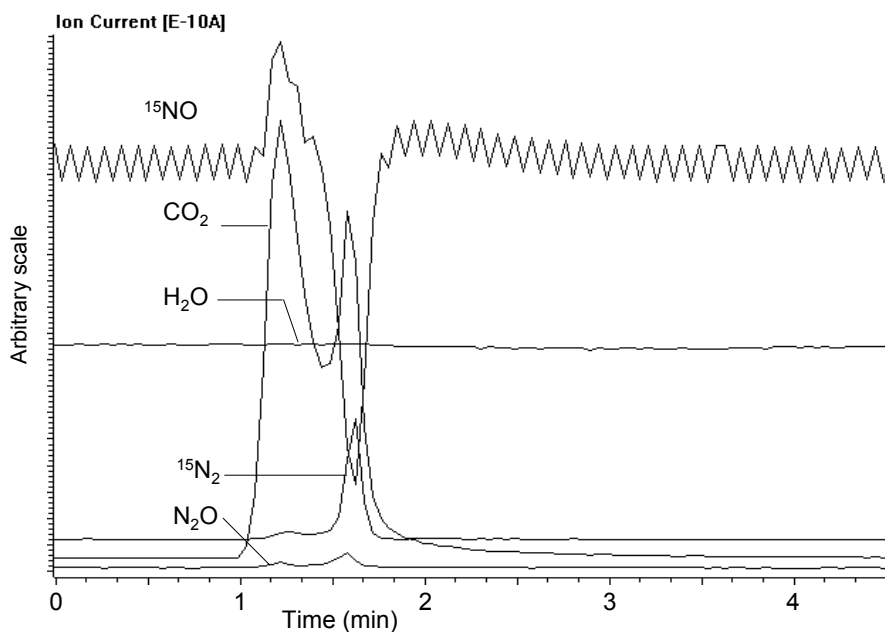
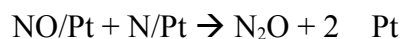
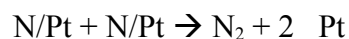
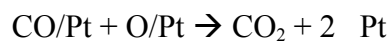
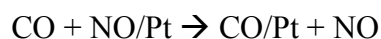


Figure 12: concentrations of the products in the gas phase out of the reactor as measured by mass spectrometry during the $^{15}\text{NO}_x$ reduction experiment on Pt/SiO_2 .

The reaction mechanism can thus be fully established:



In this case, the intermediate species CO/Pt and NO/Pt were really detected.

3) Surface of the working catalyst

The study of the surface of the working catalyst is one of the best topics for operando infrared spectroscopy. In most of the cases, the technique shows that the working catalyst in real operation conditions differs very much from the fresh catalyst. The strongest (acidic or basic) catalytic surface sites are generally very rapidly neutralised by the reactant or by side products. The surface of the operating catalyst is covered by spectator species, or by species taking part in a side or successive reactions. In some cases, this will be the normal working state, in some others it will lead to deactivation of the catalyst. On supported metal catalysts, CO and NO probe molecules will be used to characterise the oxidation state of the metal. We will discuss the examples of deactivation of an acidic zeolite by coke, the acidity change during the reaction, and the oxidation state of copper in methanol synthesis.

a) Cyclohexene conversion on HY zeolite [24]

Steamed H-Y zeolites present a rather complex spectrum in the $\nu(\text{OH})$ region. The very weakly acidic silanol groups vibrate at 3745 cm^{-1} , the acidic OH in the hypercages is at $\sim 3620\text{ cm}^{-1}$ and the one in the small cages is at ca. 3555 cm^{-1} (High Frequency and Low Frequency, resp.). The additional peak in the center, at ca. 3600 cm^{-1} , is denoted as “perturbed HF”. This is due to the perturbation of the HF OH group by extraframework phase (Lewis acid), and corresponds to a very strong site (often said superacidic), as strong as 100% sulphuric acid.

In the experiment described here, a cyclohexene flow was established over the catalyst at 640 K, and OH bands changed quickly (fig. 13). In the first seconds, the strongest acid site (perturbed HF) was affected and disappeared. HF and LF OH groups were perturbed in a second step more slowly. Simultaneously, coke bands could be observed at around 1600 cm^{-1} .

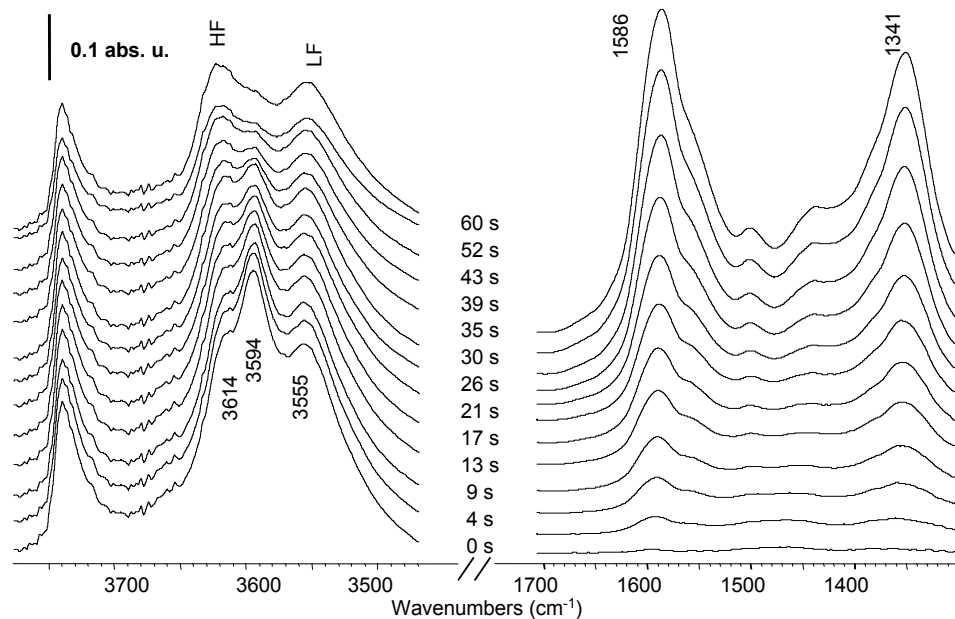


Figure 13: spectra recorded on the surface of H-Y zeolite under cyclohexene flow at 640 K.

Most OH groups disappeared after 2 min and the amount of coke increased rapidly at first, quickly reaching its maximum amount. Selectivities observed in the cyclohexene conversion reaction gave information on the various possible routes (fig. 14). Cracking and hydrogen transfer are the most demanding reactions for the acid strength and they stopped as soon as the “superacidic” sites disappeared. Isomerisation is not so demanding and could go on in the absence of any visible acidic OH.

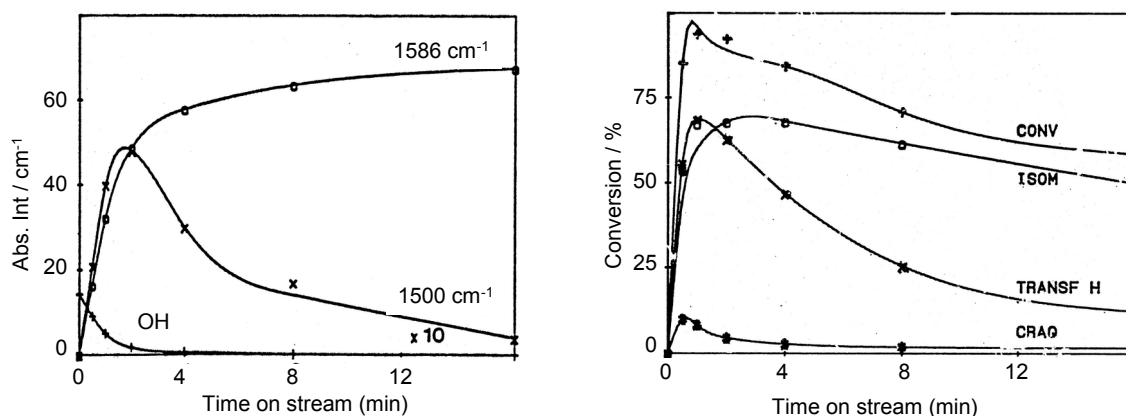


Figure 14: surface concentrations (left) compared with reaction yields (right) in cyclohexene conversion on H-Y zeolite at 650 K.

b) State of copper in the synthesis of methanol

The question of the oxidation state of copper in the synthesis of methanol had long remained open. Infrared spectroscopy was used to solve it by studying the dependence of the $\nu(\text{C}=\text{O})$ band for adsorbed CO upon the oxidation state of Cu [25]. Starting the reaction from a CO/CO₂ mixture, the maximum activity is observed at 10% CO₂ (fig. 15). The corresponding frequency for the $\nu(\text{CO})$ vibration is at 2088 cm⁻¹, indicating the coordination of most of CO to copper in the zero oxidation state.

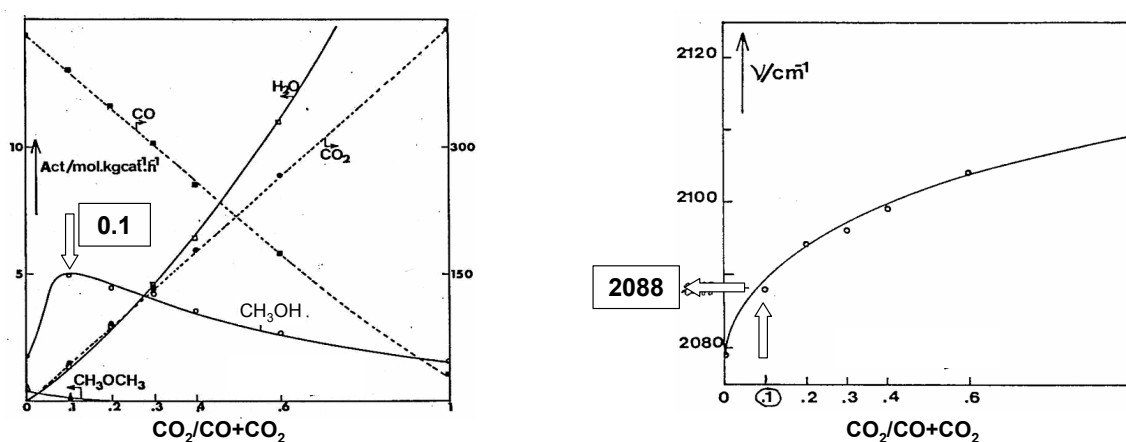


Figure 15: activity in methanol synthesis on Cu/ZnAl₂O₄ at 525 K versus CO₂/(CO+CO₂) ratio (left), and corresponding frequency observed for $\nu(\text{CO})$ (right), indicating the oxidation state of copper during the reaction.

c) Propane oxidation on modified V₂O₅ [26]

Characterising the catalyst before the reaction, when it is “clean” and has not seen any of the species in the feed, can give misleading results. In this example, the clean catalyst is mostly a Lewis type catalyst. In working conditions, water is present and transforms most of these Lewis sites into Brønsted sites, which will be the active sites in the reaction.

Modified vanadium oxide is used for the oxidation of propane into acrolein. Water in the propane flow increases the selectivity for acrolein. Infrared characterisation of the clean surface by pyridine adsorption had showed the catalyst was an acidic solid, mostly Lewis

type. Pyridine was also adsorbed *operando*, in the reaction flow in the reactor (fig. 16). The surface properties of the working catalyst were shown to be very different from those of the fresh catalyst before the reaction. In the reaction flow (or in a water flow), the amount of Lewis sites (L in fig. 16) is much lower, and the Brønsted sites (B in fig. 16) increase correspondingly (the sum remains constant). Thus, Brønsted sites are probably responsible for the production of acroleine.

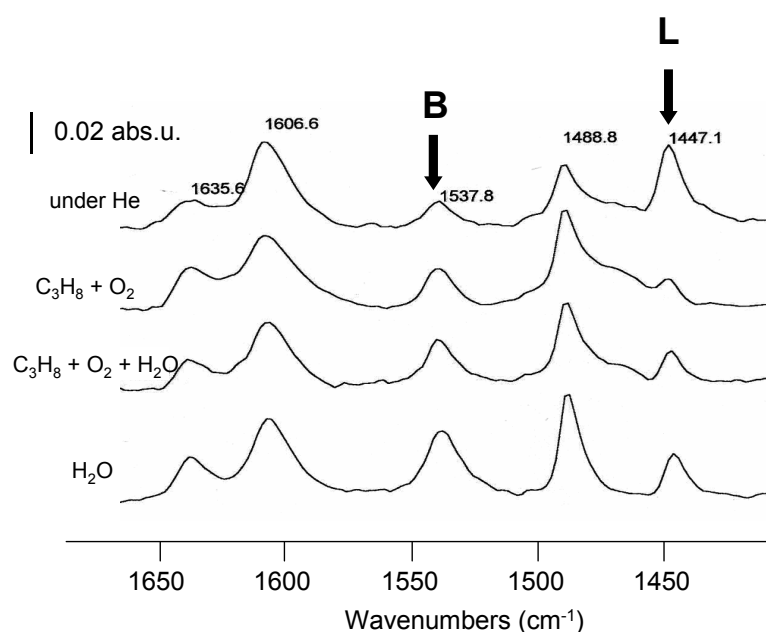


Figure 16: adsorption of pyridine on V_2O_5 at 625 K under various flow conditions.

The oxidation reaction was also performed after a pyridine pulse (fig. 17). Pyridine blocked all acid sites on the surface, and the reaction was completely stopped. After some time, pyridine desorbed, progressively restoring the Brønsted and Lewis sites on the surface. At the same time, oxidation was progressively restored to its initial level, but acroleine formation was linked to the recovering of the Brønsted sites, which was again an indication of these Brønsted sites being responsible for acroleine formation.

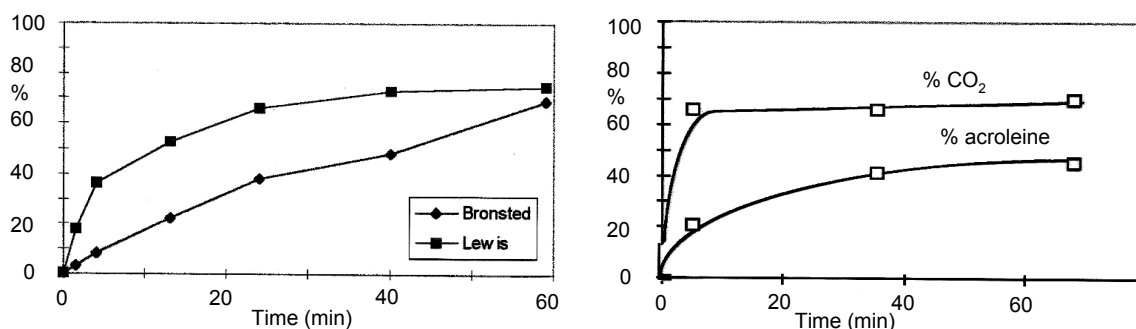


Figure 17: propane oxidation reaction on modified vanadium oxide catalyst, at 350 C. A 0.5 μ l pulse of pyridine is added to the flow at time 0. Pyridine progressively desorbs, and the Brønsted and Lewis sites are progressively recovered on the surface (left). At the same time, the reaction starts again and recovers its initial level (right).

This example clearly shows the importance of operando characterisation of catalysts. The surface of the working catalyst is not the surface of the pure and clean solid.

4) *New developments and trends*

Operando IR spectroscopy coupled with fast on-line analysis techniques (gas IR, micro GC, MS...) offers new opportunities of research in many domains:

- micro-reactivity (pulse reactivity, pulse perturbation...) to confirm the sequence of elementary reaction steps and to establish the mass balance between the surface and the gas phase
- temporal analysis of products and of surface species
- study of processes more complex than usual chemical reactors, for example automotive exhausts in alternating oxidative and reductive states (NO_x trap). This approach gives very valuable information for engine science, out of reach with other techniques.

New developments, such as chemometrics and very fast time resolution, still increase the potential of operando infrared spectroscopy in catalysis.

a) Micro-reactivity

(1) isonitriles on copper

In the selective catalytic reduction of NO_x by propane on Cu-MFI zeolite, acrylonitrile was shown to be the reaction product of NO⁺ and propene, two intermediate species in the main reaction. Acrylonitrile is further dissociated on copper to yield ethylene and isocyanide (which stays on copper) [27]. The reactivity of this NC_{Cu} species was tested by oxidation into isocyanate, NCO_{Cu}, by sending 0.4 μmol O₂ pulses on the surface [28].

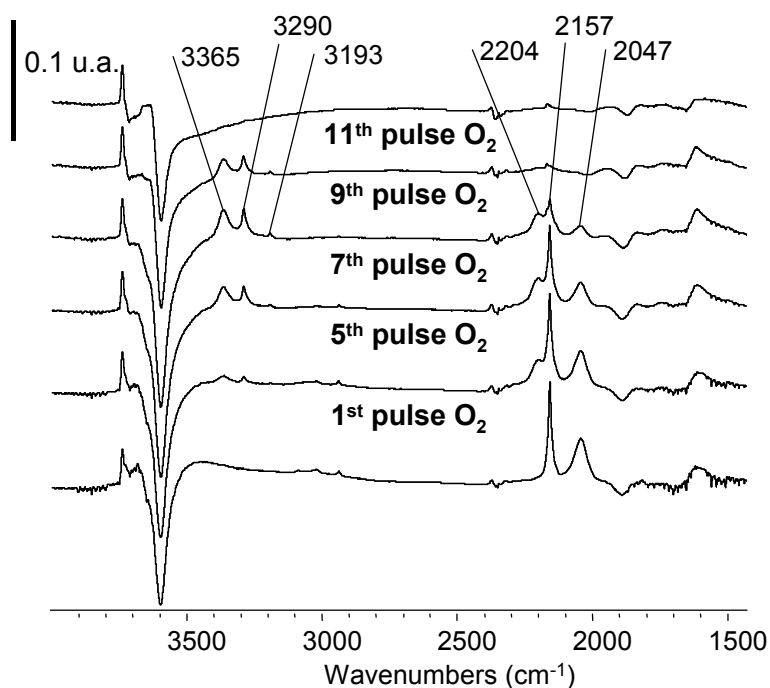


Figure 18 : changes observed for CU'NC species after sending 0.4μl O₂ pulses on the surface of Cu-MFI zeolite at 625 K.

The intensity of the band corresponding to the NC_{Cu} species (2047 cm⁻¹) decreases after each O₂ pulse, and a new band appears and increases at 2204 cm⁻¹ for the isocyanate (fig. 18). New bands also appear very soon in the 3300-3100 cm⁻¹ region for NHx_{Cu} species. After the 11th pulse, all of NC_{Cu} is oxidised and nothing remains on the surface.

On-line analysis of the gases coming out of the reactor show that the first pulses are completely consumed, while the last one gets out intact (fig. 19). Oxygen is transformed into CO₂ by hydrolysis of isocyanates:



Water is often present as traces in the helium flow and ammonia reacts further with O₂ to yield N₂. The theoretical CO₂/N₂ ratio is 2, which is in agreement with mass spectrometry (2.5).

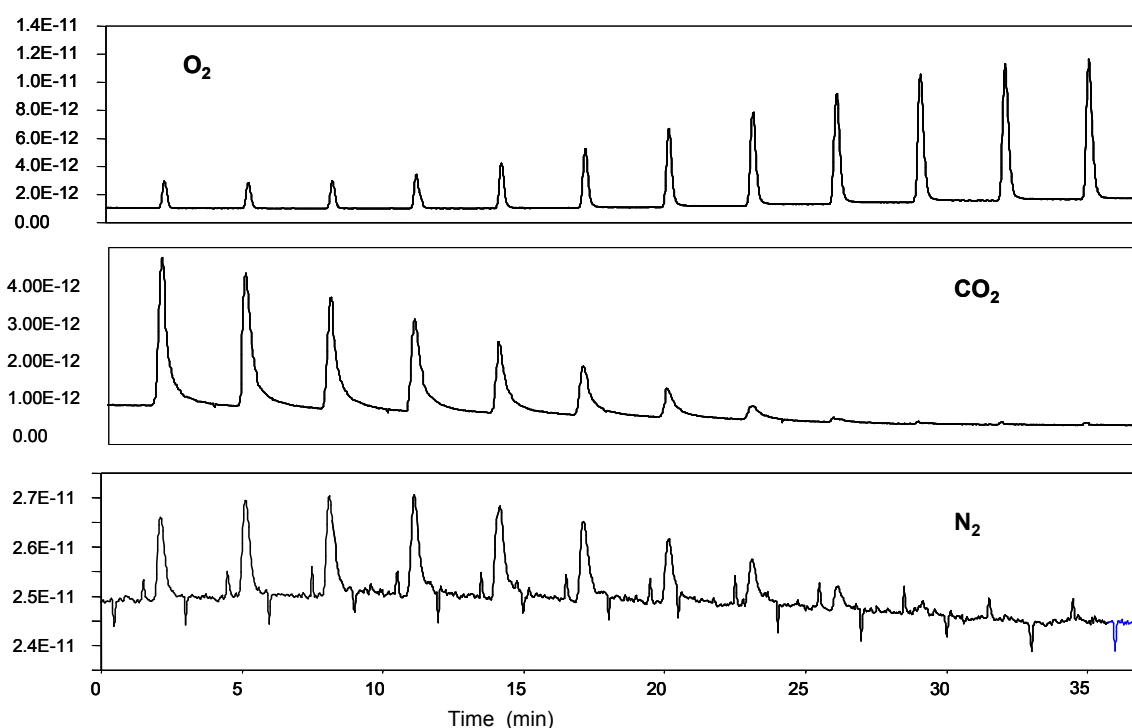
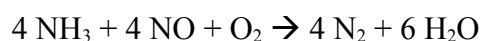


Figure 19: on-line MS analysis of gases exiting the reactor during the addition of O₂ pulses on the catalyst containing adsorbed NC_{Cu} species.

In real reaction conditions, NO is present and reacts with ammonia to form nitrogen:



This reaction was checked by preadsorbing ammonia on the catalyst before sending a NO flow in the reactor.

In this example, pulsed reaction was used to evidence the reaction mechanism. It gave successive snapshots of the reaction, like a slow motion picture of a very fast process.

(2) Alternating oxidation/reduction steps in NO_x trap.

This example is another interesting case for operando infrared, using its high time resolution. Nitrogen oxide abatement in diesel car exhausts is nearly solved in Japan, where diesel fuel only contains 5ppm sulphur with the NO_x-trap system. NO_x are trapped on the surface of the catalyst under the form of nitrates. The nitrates are rapidly reduced into nitrogen when the catalyst is saturated. In this example, platinum is used to oxidise NO in NO₂, and in the reduction step to transform nitrates into N₂. A special gas line was set on the reactor to be able to alternate oxidation and reduction conditions rapidly.

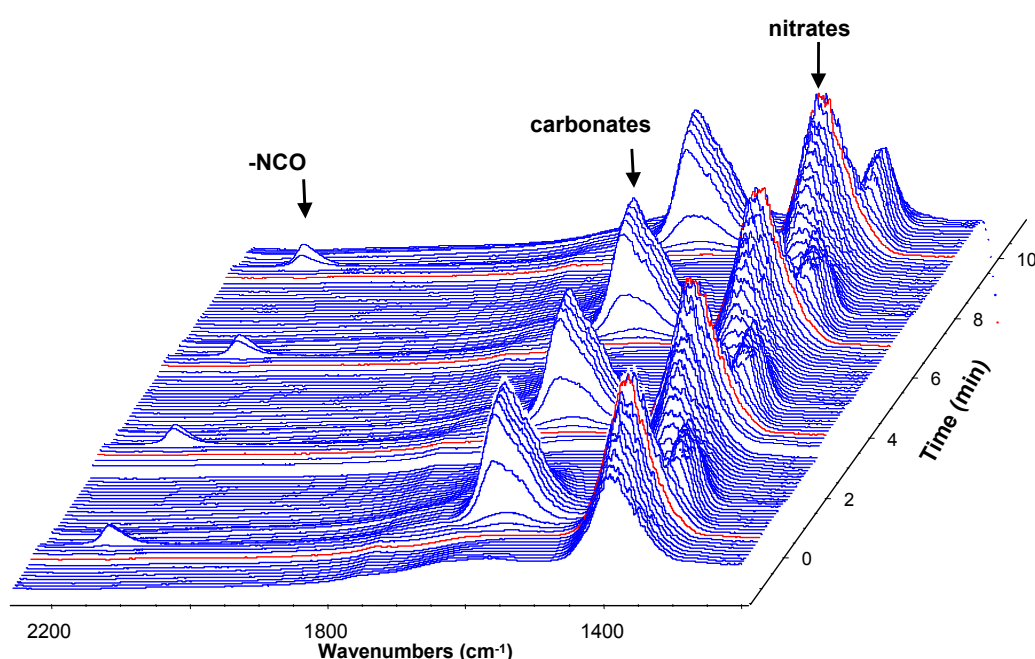


Figure 20: infrared spectra of the surface of the catalyst (Pt/Rh/BaO/Al₂O₃, Toyota type) taken every 2 s during 4 oxidation-reduction cycles. Oxidation conditions: 500 ppm NO and 10% oxygen. Reduction conditions: 0.7 % H₂, 2% CO and 0.6 % O₂, as in the exhaust of a diesel engine in hydrocarbon rich regime.

Nitrates are formed in oxidation conditions. The flow is switched to reduction conditions after 2 min, leading to the total consumption of nitrates together with the formation of surface

carbonates (production of CO_2). Isocyanates are transiently formed (2160 cm^{-1}). This time sequence is perfectly reproducible in later cycles (fig. 20).

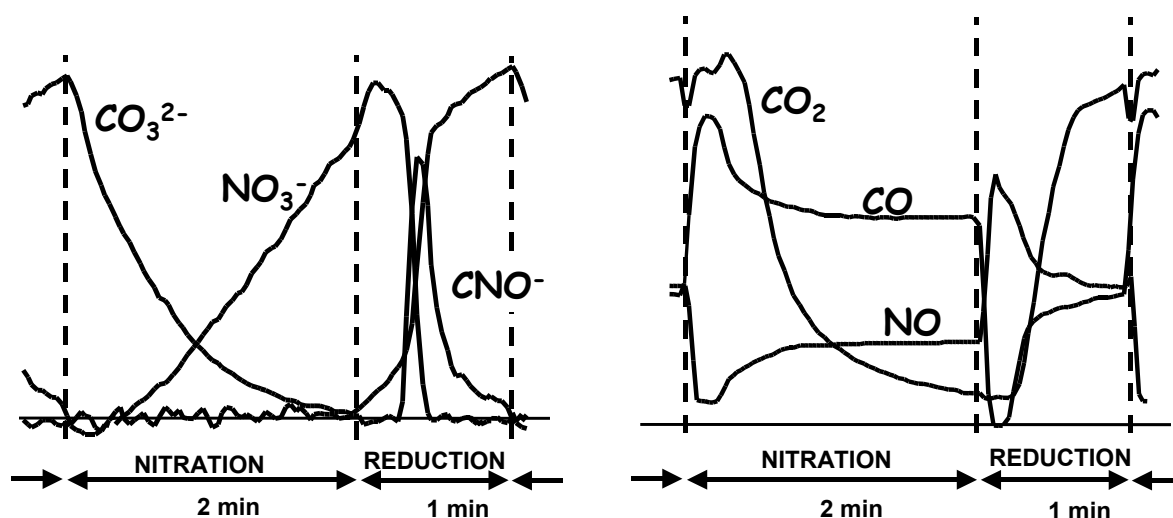


Figure 21: surface (left) and gas phase (right) concentrations during one nitration/reduction cycle, as measured by surface and gas infrared, respectively.

One of the main advantages of this approach is to be able to indicate the minimum time required for reduction of the nitrates. Minimising this time is an important point in order to reduce fuel consumption. Nitrates totally disappear in 15 s, but isocyanate needs 40 or 50 s to react, as indicated by gas phase analysis.

Nitrogen production was measured by mass spectroscopy. The MS signal at mass 28 is due to the sum of CO and N_2 in the gas phase. By comparing it with the infrared response for CO , a distortion appears during the reduction step, which is due to N_2 being produced (Fig. 22). It is in agreement with a minimum time of 50 s to evacuate NO_x under the form of N_2 . Production of N_2 takes place after the disappearing of isocyanates, which are most probably intermediates in the reduction of nitrates.

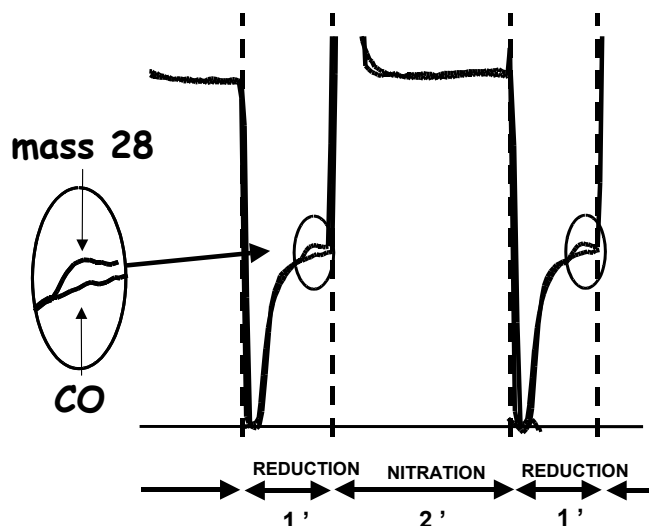


Figure 22: comparison of the infrared (CO amount) and mass spectroscopy (mass 28) to deduce the amount of N_2 produced (difference in the reduction step).

b) 2D-COS

Chemometrics will probably be one of the major developments of operando spectroscopy in the next few years. The important amount of data collected in a single experiment and the complexity of the spectra obtained in reaction conditions are often the limiting step in operando experiments. Chemometrics, on the other hand, is now a mature domain, and efforts should be taken to bring the chemometrician into the spectroscopy and catalysis laboratory. Some work has been done in the field of UV-Vis, and Principal Components Analysis was applied to in situ DRS in catalysis. Infrared is surely one of the best domains to apply these data treatment methods, since the bands are complex and many species that are observed are unknown. A first attempt has been made using 2D correlation spectroscopy (2D-COS) for the analysis of hydrocarbon reactions in zeolites.

2D-COS is a data treatment method allowing the visualisation of simultaneous or asynchronous changes in a series of spectra recorded during a perturbation (such as a chemical reaction). In most cases, bands linked by positive synchronous correlation, all changing simultaneously, come from the same chemical species. Bands linked by negative

synchronous correlation come from species whose concentrations vary in opposite directions, as in the case of one species being the product of the direct transformation of the other one. In the case of *o*-xylene isomerisation on H-MFI zeolite, 2D-COS was of great help for the assignment of cycle vibration bands to the isomers of xylene on the surface in reaction conditions [29].

Infrared bands used for distinguishing xylene isomers are located between 1300 and 1700 cm^{-1} (fig. 23). The spectra of the pure isomers in the liquid state are well known, but they are strongly modified by heating and adsorption. The spectra recorded during the isomerisation of *o*-xylene on H-MFI at 473 K were analysed by 2D-COS. The bands in the complex group around 1500 cm^{-1} were assigned based on their main contributor isomer.

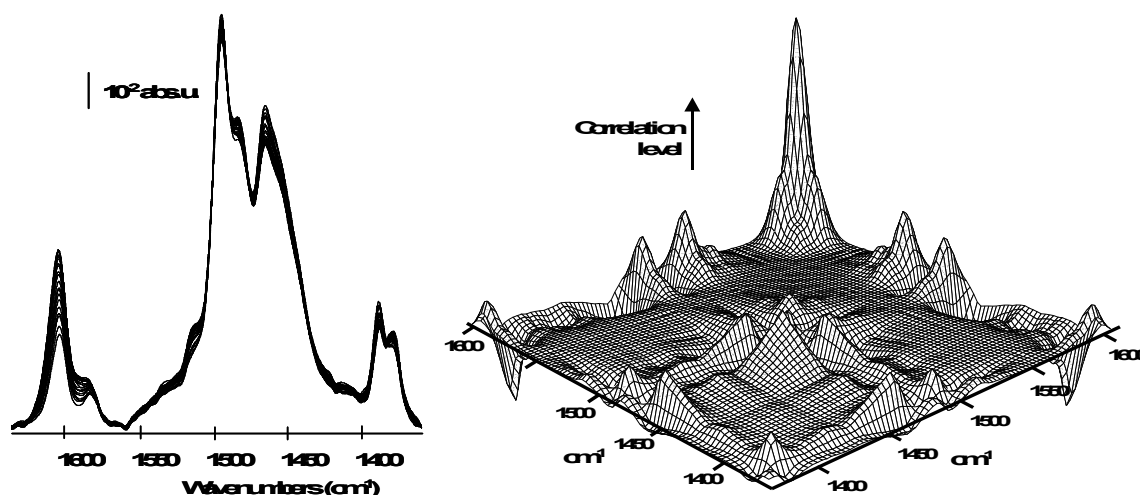


Figure 23: 1D (left) and 2D-COS spectra (right) recorded during xylene isomerisation on H-MFI zeolite.

The best bands for the quantitative monitoring of *o*- and *m*-xylene in the pores of MFI zeolite (fig. 24) could be selected (those having contribution from one isomer only), and they were not those that would have been chosen on the basis of the pure compounds spectra, due to strong influence of adsorption and reaction conditions.

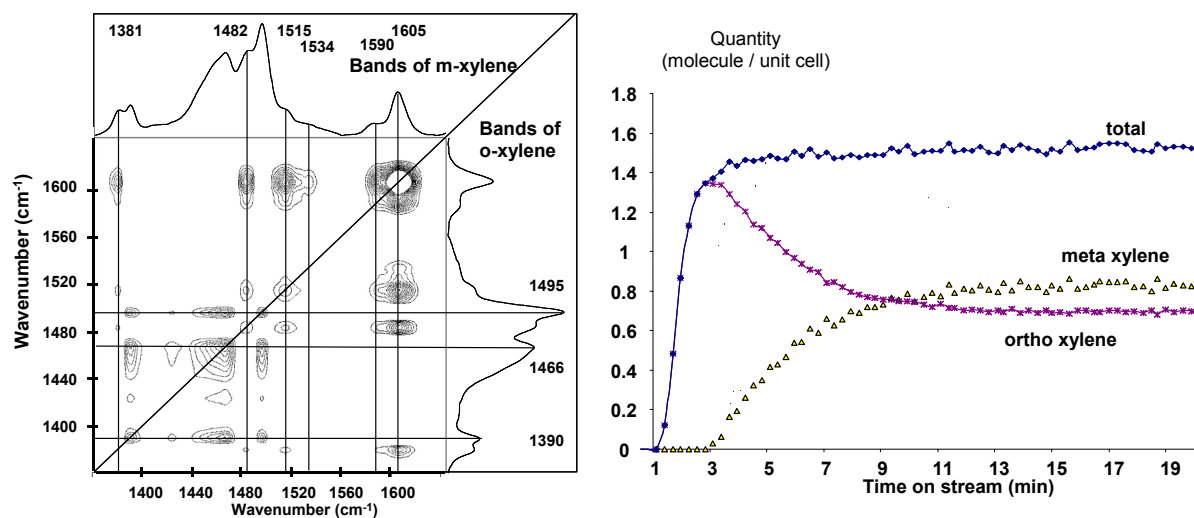


Figure 24: positive part of the synchronous 2D-COS spectrum recorded during xylene isomerisation on H-MFI zeolite at 473 K between 4 and 14 min time on stream (left), and corresponding analysis of isomers concentrations inside the zeolite pores (right).

One of the most interesting points occurred in a higher temperature experiment (573 K, fig. 25) [30]. Spectra were noisier, and although after a certain moment nothing seemed to change on the surface, the selectivity of the catalyst improved slightly with time. 2D-COS allowed the extraction of useful information out of what seemed to be only noise, and pointed at very weak coke bands appearing slowly. No correlation was detected between these coke bands and $\nu(\text{OH})$ vibrations of acidic groups. The correlation was among OH groups of extraframework phase, and with low frequency silanols groups. Using probe molecules, it was possible to determine the localisation of these low frequency silanols in the structure. Using a substituted pyridine, selective perturbation of silanols on the external surface of the crystallites was possible, and the low frequency silanols were out of reach of this bulky probe. Low frequency silanols on H-MFI are thus localised in the pore structure, but in structure defects, where the available space for coke to build up is slightly more important than in the regular pores (where coke does not form). This filling of structure defects was responsible for the improved para-selectivity of the catalyst with time on stream.

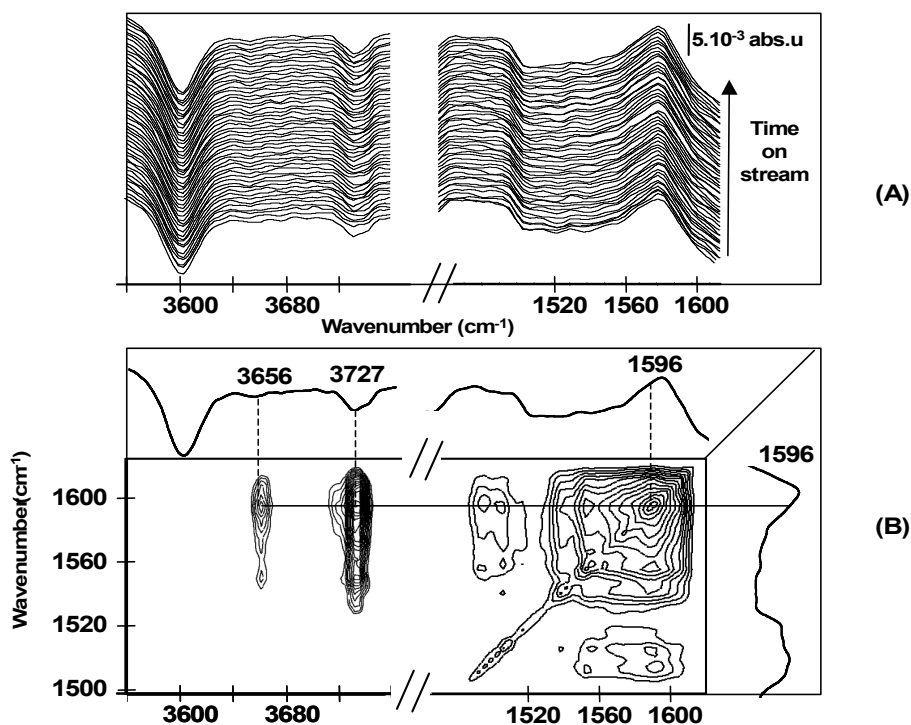


Figure 25: (A) 1D spectra collected between 5 and 60 min during *o*-xylene isomerisation on HMF1 at 573 K. (B) Corresponding 2D-COS, negative (left) and positive correlation (right).

c) Very high time resolution

Laser spectroscopy opens interesting perspectives for very high time resolution in operando infrared. Frei et al. studied the photochemistry of duroquinone in a NaY zeolite [31]. Aromatic carbonyl groups, especially in quinones, can have two excitation states, $n\pi^*$ and $\pi\pi^*$. In the $n\pi^*$ state, the double bond is severely weakened on the carbonyl group, and the reactivity is higher than in the $\pi\pi^*$ state. In the latter case, the $\nu(\text{CO})$ vibration is red shifted 100 cm^{-1} lower. Photoexcitation of quinones in a zeolite can be obtained with a laser, and short-lived excited states are formed in the pores.

Such short-lived species are out of the reach of the usual Fourier transform infrared spectrometers, as their effective time resolution is in the order of 0.1 s due to the moving mirror needed for recording the interferogram. High time resolution can be attained by step scan measurement: the mirror is stopped and the whole transient experiment is recorded and

repeated at each mirror position. Multiple scanning is then possible with the same time resolution, and the time limit is imposed by the electronics and detection rather than by the physical movement of the mirror. Here, the experiment was done with 570 successive positions for the mirror, and 25 laser shots were used and averaged at each position. It was then possible to observe, in the 50 μ s following the laser shot, the decrease of the excited species corresponding to the $\pi\pi^*$ state of duroquinone. In this example, the maximum resolution was around 100 ns (due to the time resolution of mid-infrared detectors).

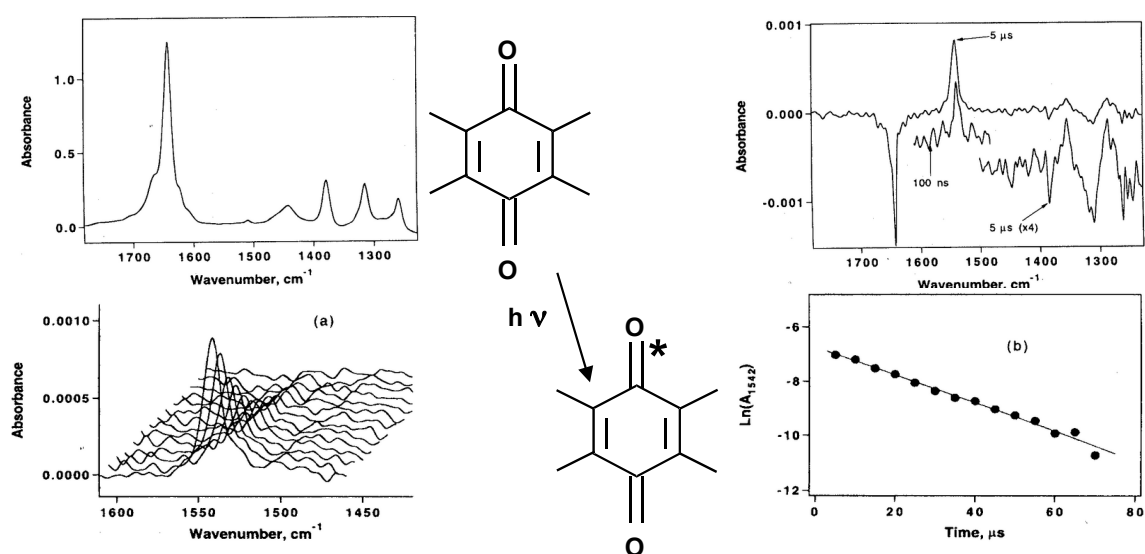


Figure 26: Top left: IR spectrum of duroquinone on NaY zeolite. Top right: changes observed after the laser shot. $\nu(\text{CO})$ is perturbed (negative band) and reappears less than 100 cm⁻¹ lower. The signal recorded during the first 100 ns after the laser shot clearly shows the shifted $\nu(\text{CO})$ band. Bottom: decrease of the excited state with time (adapted from ref. 31, with permission).

This method opens very interesting perspectives for the detection of very short-lived species on surfaces, and has been applied by Frei's group to photochemistry [32, 33], which is reversible and reproducible, both seen as key features for step-scan interferometry.

High time resolution can also be reached by laser spectroscopy, without interferometry, by pump probe experiments. A laser is used for the excitation of a particular vibration level and the infrared absorbance of the sample is probed by a second weaker laser pulse. By tuning the

probe laser, the spectrum can be explored in the frequency range, while the variation of the spectrum with time is obtained by adjusting the delay between pump and probe. This method has been used to study dynamics of H-bond dissociations, as for example for methanol adsorbed (by H-bonding) on H-Y zeolites [34]. This is a first step toward the time resolved observation of a non-photochemical reaction started by a laser pulse, and might be a possible future for operando spectroscopy [35].

Conclusions

We have seen the importance of studying the catalyst in working conditions rather than the clean activated solid. This is only possible with operando spectroscopy, and infrared is one of the major tools in the domain. Due to its long lifecycle, infrared operando is now a mature technique, and a lot of information on the mechanism of the surface reaction can be obtained.

A systematic and practical approach of operando infrared study of heterogeneous catalysis is not only possible, it can also be rigorous and comprehensive. The study of a catalytic reaction by operando infrared is decomposed in three steps:

- determination of surface species and assignment of infrared bands
- identification of intermediate and spectator species
- characterisation of the surface and of the active sites of the working catalyst.

In the examples given here, the various possible ways for these three steps have been shown. From the deactivation of the active sites by coke to the kinetic determination of the surface reaction mechanism, most of the aspects of the catalytic reaction can be studied, and sometimes completely determined and understood. New techniques, increasing the time resolution or helping with data treatment, will still improve the efficiency of operando infrared. Due to the great complexity of the observed phenomenon and the important number

of surface species detected, great care should be taken not to overlook any of the steps of the study. In addition, the results obtained by all the analysis techniques have to be combined and examined together. The surface concentrations can be measured during the reaction, and the kinetic analysis of the dynamic behaviour of the chemical reactor (e.g. for microkinetics) should not be performed without taking it into account. In the future, other spectroscopic techniques like NMR, Raman and EXAFS could be combined with infrared to get an overall picture of the chemical process, including structural and atomic modifications.

Bibliography

- 1 - Baddour, R.F., Modell, M., Goldsmith, R.L., *J. Phys. Chem.*, **74**, 1787-96 (1970).
- 2 - Ryczkowsky, J., *Catal. Today*, **68**, 263-81 (2001).
- 3 - Weckhuysen, B.M., *Chem. Commun.*, 97-110 (2002).
- 4 - Almusaiter, K., Krishnamurthy, R., Chuang, SSC., *Catal. Today* **59**, 365-71 (2000).
- 5 - Burcham, L.J., Badlani, M., Wachs, I.E., *J. Catal.*, **203**, 104-21 (2001).
- 6 - Dardas, Z., Süer, M.G., Ma, Y.H., Moser, W.R., *J. Catal.*, **159**, 204-11 (1996).
- 7 - Ferri, D., Bürgi, T., Baiker, A., *J. Phys. Chem. B*, **105**, 3187-95 (2000).
- 8 - Hicks, R.F., Kellner, C.S., Savatsky, B.J., Hecker, W.C., Bell A.T., *J. Catal.*, **71**, 216-18 (1981).
- 9 - Jung, K.D., Bell, A.T., *J. Catal.*, **193**, 207-23 (2000).
- 10 - Haneda, M., Morita, T., Nagao, Y., Kintaishi, Y., Hamada, H., *PCCP*, **3**, 4696-700 (2001).
- 11 - Anderson, J.A., Khader, M.M., *J. Mol. Catal. A: Chem.*, **105**, 173-83 (1996).
- 12 - Karge, H.G., Niessen, W., Bludau, H., *Appl. Catal. A: Gen.*, **146**, 339-49 (1996).
- 13 - Vimont, A., Thibault-Starzyk, F., Lavalley, J.-C., *Stud. Surf. Sci. Catal.*, **130**, 2963-2969 (2000).
- 14 - Vimont, A., Marie, O., Gilson, J.-P., Saussey, J., Thibault-Starzyk, F., Lavalley, J.-C., *Stud. Surf. Sci. Catal.*, **126**, 147-154 (1999).
- 15 - Centi, G., Perathoner, S., Tonini, S., *Catal. Today*, **61**, 211-21 (2000).
- 16 - Amblard, M. Burch, R., Southward, B.W.L., *Catal. Today*, **59**, 365-71 (2000).
- 17 - Ortelli, E.E., Wambach, J., Wokaun, A., *Appl. Catal. A: Gen.*, **192**, 137-52 (2000).
- 18 - Miners, J.H., Martin, R., Gardner, P., Nalezinsky, R., Bradshaw, A.M., *Surf. Sci.*, **377**, 791-5 (1997).
- 19 - Chafik, T., Dulaurent, O., Gass, J.L., Bianchi, D., *J. Catal.*, **179**, 503-14 (1998).
- 20 - Maetz, P., Saussey, J., Lavalley, J.C., Thouroude, R., *J. Catal.*, **147**, 48-56 (1994).
- 21 - Audry, F., Hoggan, P.E., Saussey, J., Lavalley, J.-C., Lauron-Pernot, H., Le Govic, A.-M., *J. Catal.*, **168**, 471-81 (1997).
- 22 - Le Peltier, F., Chaumette, P., Saussey, J., Bettahar, M.M., Lavalley, J.C., *J. Mol. Catal. A : Chem.*, **122**, 131-9 (1997).
- 23 - Freysz, J.-L., Saussey, J., Lavalley, J.-C. Bourges, P., *J. Catal.*, **197**, 131-138 (2001).

- 24 - Joly, J.F., Zanier-Szydowski, N, Colin, S., Raatz, F., Saussey, J., Lavalley, J-C., *Catal. Today*, **9**, 31-38 (1991).
- 25 - Saussey, J., Lavalley, J.C., *J. Mol. Catal.*, **50**, 343 (1989).
- 26 - Savary, L., Saussey, J., Costentin, G., Bettahar, M.M., Lavalley, J.C., Gubelmann-Bonneau, M., *Catal. Lett.*, **38**, 197-201 (1996).
- 27 - Poignant, F., Freysz, J.L., Daturi, M., Saussey, J., *Catal. Today*, **70**, 197-211 (2001).
- 28 - Poignant, F., Freysz, J.L., Daturi, M., Saussey, J., Lavalley, J.C., *Stud Surf. Sci Catal.*, **130**, 1487-92 (2000).
- 29 - Thibault-Starzyk, F., Vimont, A., Fernandez, C., Gilson, J.-P., *Chem. Commun.*, 1003-1004 (2000).
- 30 - Vimont, A., Gilson, J.P., Thibault-Starzyk, F., *Catal Today*, **70**, 229-243 (2001).
- 31 - Sun, H., Frei, H., *J. Phys. Chem. B*, **101**, 205-209 (1997).
- 32 - Blatter, F. Sun, H., Vasenkov, S., Frei, H., *Catal. Today*, **41**, 297-309 (1998).
- 33 - Ulagappan, N., Frei, H., *J. Phys. Chem. A*, **104**, 7834-9 (2000).
- 34 - Bonn, M., van Santen, R.A., Lercher J.A., Kleyn, A.W., Bakker, H.J., *Chem.Phys.Lett.*, **278**, 213-9 (1997).
- 35 - Bonn, M., Kleyn, A.W., Kroes, G.J., *Surf. Sci.*, **500**, 475-99 (2002).